Rh atom ejection from keV ion-bombarded $p(2\times2)$O/Rh{111}: Adsorption site and coverage determination from angle-resolved desorption measurements

C. T. Reimann,[a] M. El-Maazawi, K. Walzl, B. J. Garrison,[b] and N. Winograd
Department of Chemistry, The Pennsylvania State University, University Park, Pennsylvania 16802
D. M. Deaven[c]
Department of Physics, The Pennsylvania State University, University Park, Pennsylvania 16802

(Received 1 September 1988; accepted 19 October 1988)

Angular distributions of Rh atoms desorbed by energetic ion bombardment of an oxygen covered Rh{111} surface are measured accurately using a multiphoton resonance ionization (MPRI) detection technique. The results, in conjunction with molecular dynamics calculations of the ion impact event show that these distributions reflect the near-surface crystal structure. The molecular dynamics calculations were performed using a many-body embedded-atom potential to describe the dynamics of the Rh atoms and a pair-wise additive potential to describe the oxygen–Rh interactions. Several oxygen overlayer structures were considered for molecular dynamics modeling of the desorption process, including $p(2\times2)$ overlayers with a coverage of 0.25 monolayer (ML), and $p(2\times1)$ overlayers with a coverage of 0.50 ML, both of which are consistent with low energy electron diffraction (LEED) data. Three different adsorption sites were tested: threefold symmetric sites over second layer Rh atoms, threefold symmetric sites over third layer Rh atoms, and atop sites. The calculated azimuthal angular distributions of desorbed Rh atoms for each of these cases are unique, matching the experimental data best in the case of a $p(2\times1)$ overlayer with oxygen atoms adsorbed in threefold symmetric sites over third layer Rh atoms. The calculated Rh atom desorption yield (ejected atoms per incident ion) is sensitive to the oxygen coverage in the range 0.25–0.50 ML. These calculations are important in developing a surface bonding site and coverage consistent with LEED and our experiments. The peak in energy distribution of ejected Rh atoms from the oxygen covered surface is at a lower energy value than that of the clean metal. This indicates that collisional energy loss processes contribute to determining the peak position as well as the well known binding energy effect.

I. INTRODUCTION

A fundamental goal in surface science is to determine the structure of surface layers, and to evaluate the atomistic nature of the binding sites, coverage, and possible ordering of adsorbate overlayers. Although surface structure information is available through a variety of techniques such as low energy electron diffraction current–voltage (LEED *I–V*) analyses and surface extended absorption fine structure (SEXAFS) measurements, ion beam techniques can provide detailed structural information through the powerfully simple concepts of atom channeling and blocking.[1–4] Recently, detailed measurements of target particle desorption by incident low kinetic energy (KE) heavy ions have been described for Rh{111}.[5–8] The KE and angular distributions of desorbed Rh atoms, when combined with classical dynamical calculations of the ion impact event based on a potential developed using the embedded atom method (EAM), have been shown to reflect the details of the surface structure. The structure sensitivity arises because ejecting atoms are channeled and blocked in particular azimuthal directions along the crystal surface. This hypothesis suggests that if desorption mechanisms are adequately understood, surface structure can be obtained from careful measurements of desorption phenomena.

Angle-resolved secondary ion mass spectrometry (SIMS) in which ejected ions are detected has already provided solutions to certain surface structure problems.[2–4,9,10] There are advantages, however, to measuring the distributions of desorbed neutral species. The desorbed particles from metals are largely neutral. Moreover, detection of neutral atoms minimizes the matrix effects that plague quantitative SIMS.[11] From a theoretical point of view classical dynamics calculations of the desorption process, important to achieving an overall understanding of desorption mechanisms, are more readily compared to experimental data when desorption of neutral species rather than that of ions is measured.[12] In order to measure neutral atom desorption, a high efficiency detector based on multiphoton resonance ionization (MPRI) of the desorbed species has been recently developed. This detector simultaneously allows kinetic energy- and angle-resolved neutral (EARN) desorbed atom distributions to be accurately measured.[13] The detailed picture

[a] Current address: Naval Research Laboratory, Washington, D.C. 20375.
[b] Camille and Henry Dreyfus Teacher–Scholar.
[c] Current address: Department of Physics, University of California, Berkeley, CA 94720.

 0021-9606/89/032027-08$02.10

of the desorption phenomena that this detector provides is an invaluable aid to understanding desorption mechanisms and relating these measurements to surface structure.

We have chosen to focus on the adsorption of oxygen on Rh{111} in order to rigorously test the sensitivity of measured Rh angular distributions to the specific nature of the oxygen atom binding site. Many previous experiments have been performed on this system. In temperature programmed desorption (TPD) experiments, the dependence of the temperature for molecular oxygen desorption on initial oxygen exposure indicates that this desorption is a second order process, strongly suggesting dissociative adsorption.[14] Experiments involving isotopes of oxygen establish directly that a large fraction of adsorbed molecular oxygen dissociates on Rh{111}, even at temperatures as low as 100 K.[15]

The ordering and coverage of oxygen overlayers on Rh crystals have been extensively examined. Early LEED studies were interpreted as indicating that oxygen forms a $p(2\times2)$ structure on the {111} face of Rh and on several other transition metal surfaces.[14] This structure is shown in Fig. 1(a). Based on "streaking" of LEED spots observed under certain low temperature deposition conditions, it was suggested that on Rh{111}, oxygen actually forms three rotated domains of a $p(2\times1)$ structure, which under room temperature deposition conditions would yield a $p(2\times2)$ LEED pattern.[16] One domain of the $p(2\times1)$ structure is shown in Fig. 1(b). The simplest $p(2\times2)$ overlayer has a coverage of 0.25 ML, but the simplest $p(2\times1)$ overlayer has a coverage of 0.50 ML. In another study, the saturation oxygen atom coverage was found to be even higher, 0.83 ML.[17] This higher coverage was determined by an x-ray photoelectron spectroscopy (XPS) comparison of oxygen coverage on Rh{111} to that on Pt{111}, where the latter coverage was independently verified to be 0.25 ML.[18] Oxygen atoms also form an ordered overlayer on Ni{111} with a coverage of 0.25 ML.[19]

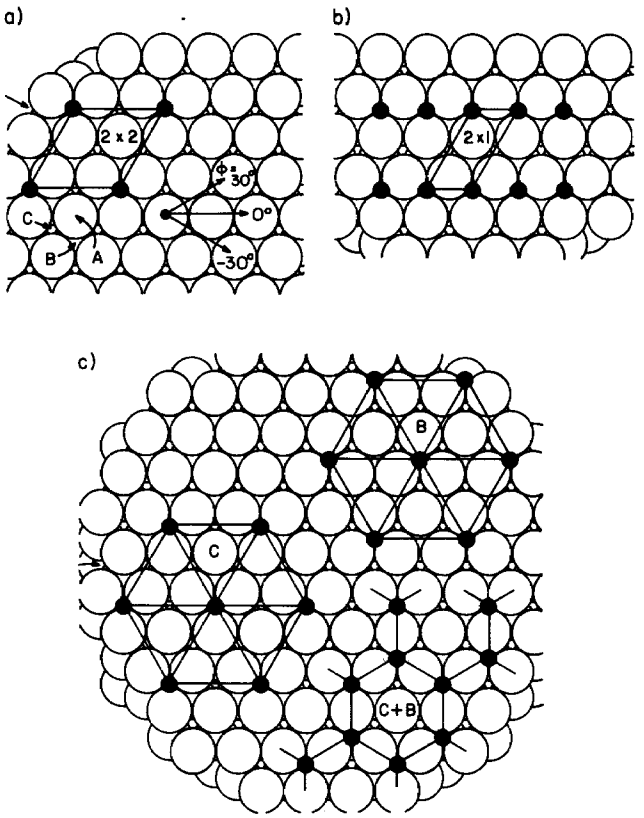

FIG. 1. The structure of the Rh{111} lattice and possible oxygen atom overlayer superstructures. (a) Definition of the azimuthal angles, view of three high-symmetry atomic adsorbate sites, and view of a $p(2\times2)$ superstructure; (b) view of a $p(2\times1)$ superstructure; (c) view of $p(2\times2)$ superstructures in which oxygen atoms occupy the C site and the B site; and a "graphitic" superstructure in which oxygen atoms occupy both C and B sites.

Binding site information may be obtained by using dynamical LEED analysis. Three possible high symmetry binding sites on {111} surfaces, an atop site and two threefold hollow sites [Fig. 1(a)], have been examined with this analysis. These configurations are shown in Fig. 1(a). The atop site is referred to as the A site, the threefold hollow over a second layer Rh atom is referred to as the B site, and the threefold hollow over a third layer Rh atom is referred to as the C site. In an early study of the $p(2\times2)$ overlayer of oxygen atoms on Ir{111}, it was concluded that oxygen atoms bond in the C site.[20] The only detailed dynamical LEED study of the O/Rh{111} system assumes either a $p(2\times2)$ structure with oxygen atoms in either the C site or the B site, or else a "graphitic" overlayer in which both types of sites are occupied [Fig. 1(c)].[21] The best dynamical LEED fit was obtained assuming a simple $p(2\times2)$ overlayer with oxygen atoms in the C site.[21] However, in view of other evidence suggesting that an oxygen coverage corresponding to a $p(2\times1)$ overlayer is in fact expected, the precise geometry of the O/Rh{111} system is not yet elucidated.

We have applied the EARN technique to the O/Rh system.[5–7] Preliminary EARN distributions from oxygen-covered Rh{111} were distinctly different from those found from clean Rh{111}.[6,7] Upon oxygen adsorption, the total ejection yield of Rh atoms is reduced by a factor of about 2, the azimuthal distributions of ejected Rh atoms are altered, and the peak in the polar angle distribution occurs closer to the normal direction of the crystal. Based on the idea that oxygen atoms bound to the surface in specific sites would preferentially block Rh atoms ejecting in certain directions, these data were interpreted as indicating that oxygen atoms bind in the C sites. Preliminary calculations were attempted in which pairwise additive potentials were employed to model a Rh microcrystallite with a $p(2\times2)$ oxygen atom overlayer.[6] The assumption of the C site led to marginally better agreement with the data than the assumption of the A site.

In this paper, we present recently obtained, detailed EARN distributions from clean and oxygen-covered Rh. We also develop a novel approach to classical dynamics calculations of the ion impact event using an EAM[8] potential to bind together a model Rh microcrystallite and pair potentials to bind oxygen atoms to this crystallite. In the calculations, several trial geometries are assumed. These trial structures include both $p(2\times2)$ and $p(2\times1)$ overlayers, with oxygen adsorbed in either the A, B, or C sites. After detailed comparison between these new calculations and those performed on clean Rh{111},[8] we conclude that a $p(2\times1)$ overlayer with oxygen atoms adsorbed in the C sites yields the best agreement with the experimental data. We have thus

confirmed our earlier ideas about the simple but powerful relation between surface bonding site and coverage and the angular distributions of atoms desorbed from single crystal surfaces by keV ion bombardment. The channeling and blocking interactions between an ejecting atom and its immediate neighbors, essentially determined by the local surface structure, strongly influence the directions in which atom ejection is probable. Adatom binding sites may therefore be uniquely identified by their directionally dependent blocking of escaping substrate atoms. The adsorption of oxygen causes the peak in the Rh atom energy distribution to shift to a lower value in both the experimental and calculated Rh atom distributions. This indicates that collisional energy loss mechanisms are more important than surface binding energy effects in influencing the peak in the energy distribution.

II. EXPERIMENTAL METHOD

The experimental apparatus has been discussed in detail elsewhere.[13] Briefly, the experiments are performed in a cryopumped ultrahigh vacuum (UHV) system with a base pressure of 2×10^{-10} Torr. The UHV chamber is composed of two levels, one containing LEED/Auger spectroscopy, and one containing apparatus for performing sputter cleaning and laser-based detection of desorbed atoms. Samples are mounted to a precision manipulator capable of vertical, horizontal, polar, and azimuthal motions. The manipulator is equipped with an electron-beam heater for sample annealing, and the temperature is monitored with a chromel–alumel thermocouple spot welded to the sample holder.

A Rh single crystal was oriented to within $\pm 0.5°$ of the {111} face by Laue backreflection and was then polished with diamond paste. The crystal was cleaned *in situ* by extensive sputter/anneal cycles coupled with catalytic removal of surface-segregated carbon via oxygen treatment at elevated temperatures.[22] A $\sim 2\ \mu A/cm^2$, 5 keV Ar^+ ion beam was employed for sputter cleaning. The crystal was annealed at ~ 870 °C. Surface-segregated carbon was removed by exposing the crystal to an oxygen pressure of $\sim 2\times10^{-7}$ Torr at a temperature of 650 °C. Before LEED or MPRI experiments were performed, the crystal was flashed to ~ 1000 °C and then cooled to room temperature. Excellent (1×1) LEED patterns were observed after this treatment.

Oxygen overlayers were obtained by exposing the crystal to 20 Langmuir (L) of oxygen at $\sim 1\times10^{-7}$ Torr. This results in a $p(2\times2)$ LEED pattern commonly observed on oxygen-exposed {111} transition metal surfaces.[14] The base pressure of the system was sufficiently low that codeposition of impurities during overlayer adsorption was not a problem as observed by others.[23] Flashing the crystal to ~ 900 °C resulted in a return to the (1×1) LEED pattern and to the EARN data characteristic of clean Rh{111}. After extensive cleaning, it was possible to observe excellent (2×2) LEED patterns after only ~ 5 L exposure to oxygen, but most of the experiments were completed using 20 L exposures. While the EARN data changed rapidly during the first 5 L of exposure, they remained constant thereafter.

A focused, pulsed 5 keV Ar^+ ion beam is employed to desorb neutral Rh atoms from a Rh{111} crystal, and detection of these atoms is accomplished by MPRI. A Nd:YAG-pumped dye laser with a frequency doubler, operating at 312 nm, is employed to ionize the desorbed atoms. The laser is focused into a thin ribbon and is directed ~ 1 cm in front of the crystal, and photoions are extracted onto a multichannel-plate (MCP) detector and a phosphor plate. A TV camera interfaced to an LSI-11/23 minicomputer records the photoion signal. The photoion extraction potentials and the MCP are gated in order to minimize spurious signals from secondary ions and from stray laser light. However, there is still a noticeable secondary ion signal which is measured and subtracted. Polar angle resolved measurement of desorbed atoms is accomplished at polar ejection angles in the range $\theta = 0°$ (normal ejection from the crystal) to $\theta = 90°$ (grazing ejection). Since the ion and laser beams are pulsed, a time-of-flight (TOF) measurement of KE can be performed on the desorbed netural atoms. For a given delay between the incident ion and ionizing laser pulses, each polar angle corresponds to a different KE. Thus, the experiment is performed at many delay times and a software procedure deconvolutes the KE and polar angle information. The MPRI-based EARN experiment is sufficiently sensitive that the data are accumulated using low ion fluence, and therefore there is negligible surface damage during the experiment.

We have examined primarily the $\phi = 0°$ and $\phi = \pm 30°$ azimuths in our experiments. A separate measurement must be performed in order to obtain information about atom ejection along each of the azimuths. LEED is used to orient the crystal to the $\phi = 0°$ azimuth, and distinguishing between $\phi = \pm 30°$ is accomplished through comparison of clean Rh{111} EARN distributions with the results of classical dynamics calculations. These azimuths are defined in Fig. 1. The data were reproducible to within about 20%. Because of some variation in the data that occurred from day to day, we have chosen to compare data on the O/Rh system only with data from clean Rh taken on the same days. Thus, the data from clean Rh displayed below differ slightly from the data published previously.[6,8]

III. CLASSICAL DYNAMICS CALCULATIONS OF THE ION-IMPACT EVENT

Classical dynamics calculations are important to our understanding of keV ion-induced desorption. This importance arises because the essential feature of the desorption event, the collision cascade, is quite complex.[24] Another reason we rely on classical dynamics calculations to enhance our understanding is that in the present experiment, we examine Rh atoms ejected from underneath an oxygen overlayer, rather than examining the ejected O atoms. In a typical adsorbate overlayer, the relative coverage is less than one monolayer, which means that different Rh atoms can have different local environments. The complexity of the surface from the point of view of the Rh atoms adds to the necessity for doing classical dynamics calculations to understand the Rh ejection process.

Classical dynamics calculations of ion-induced desorption are performed using assumed potentials which bind together the atoms in a model crystallite and which describe

how incident ions interact with atoms in the crystallite. Once these potentials are delineated, Hamilton's equations of motion are integrated numerically to determine the erosional effect of ion impact. Currently we have two types of binding potentials at our disposal: the pairwise interaction potential[6] and an interaction potential based on the embedded atom method (EAM).[8] In the EAM, the potential energy of the ith atom in the lattice is written as[25,26] $U_i = F(\rho_i) + \frac{1}{2}\Sigma_{j\neq i}\,\varphi(r_{ij})$. In this expression, ρ_i is the total electron density at the position of the ith atom, F is a nonlinear function, and φ is the potential energy of repulsion between the ion cores of the ith and jth atoms separated by a distance r_{ij}. The electron density at the position of atom i is given by $\rho_i = \Sigma_{j\neq i}\,\rho_{\rm at}\{|\mathbf{r}_j - \mathbf{r}_i|\}$, the sum of the atomic electron densities $\rho_{\rm at}$ contributed by the surrounding atoms. Although the form of the EAM potential can be derived from density functional theory,[27] the EAM is still empirical in nature. Also, an alternate interpretation exists for ρ_i.[28] This parameter may represent the local density of atoms[28] rather than the local electron density.[25,26] In either interpretation, however, the atomic interactions are clearly the consequence of many-body forces, which more realistically model a metal than the assumption of pairwise-additive potentials.[6] The EAM[8] accounts for the peak features in the angular and KE distributions better than the pair-potential method.[6]

In order to calculate particle ejection from the O/Rh system, it would be desirable to incorporate the oxygen overlayer atoms into the EAM formalism. Unfortunately, it is not yet known how to accomplish this incorporation. Therefore, pair potentials continue to be used in order to bind oxygen atoms to the Rh crystallite surface. The O/Rh interaction[6] is modeled by a Morse potential splined to a Molière potential with a screening radius of 0.9 times the Firsov value[29] at internuclear separation below $\sim$0.757 Å [Table I(R_a)]. The binding energy of an O atom is set equal to $0.5\times\{2.43 + 5.21\ \text{eV}\} = 3.82$ eV, where 5.21 eV is the dissociation energy of molecular oxygen, and 2.43 eV is the activation energy of molecular oxygen desorption from Rh{111}.[30] The oxygen–metal atom bond length in this situation is close to what is predicted assuming a bond order of 0.67, appropriate for divalent oxygen associating with three metal atoms.[21,31] For the atop site, the oxygen was assumed to bind 1.95 Å above the surface plane. This value is chosen as the sum of the approximate atomic radii of Rh and O atoms[6] (and is close to the Rh–O distance assumed in the case of the B and C sites). The range parameter α in the Morse potential is selected so that the Morse potential splines well to a Molière potential with a screening factor of 0.9 times the Firsov screening length, and so that there is no net force on the atom. For the O–O interaction a Morse potential is used. The Morse parameters[6] approximated from diatomic molecular constants are $\alpha = 2.65$ Å^{-1}, $R_{\rm eq} = 1.21$ Å, and $D_e = 5.21$ eV. These tentatively chosen potentials given in Table I form a good starting point for doing classical dynamics calculations. The Ar–Rh and Ar–O interactions were described by Molière potentials with the full Firsov screening length.[29]

TABLE I. Rh–O interaction potentials.[a]

	D_e(eV)	R_e(Å)	a(Å^{-1})	R_a(Å)	R_b(Å)	R_c(Å)
A site	1.702	2.095	1.8	0.757	1.407	4.565
B,C sites	0.97	2.01	2.2	0.757	1.407	4.565

[a] See Ref. 6 for the functional forms.

The Rh crystallite consists of five layers of {111} planes, each approximately circular, and each containing 105 atoms.[6,8] This size is assumed to be adequate because less than 10% of the ejected atoms come from the edge of the crystallite. In the simulation the aiming points of the primary particle on the surface are chosen from a region in the center of the crystal that represents the symmetry of the infinite system. Although the experiment employed 5 keV Ar^+ ions, the simulations were performed with 3 keV ions in order to reduce the size of the model crystallite. We do not feel that this is a serious approximation as the majority of the ejection events in the 5–50 eV range arise from Rh–Rh and Rh–O interactions and not directly from Ar–Rh collisions.

IV. RESULTS AND DISCUSSION

A summary of polar angle distributions of Rh atoms ejected from clean and oxygen-exposed Rh{111} is shown in Fig. 2. The data from clean Rh{111} exhibit trends described elsewhere.[6,8] Briefly, Rh atom ejection is focused into a polar angle of about $\theta = 40°$. Ejection is concentrated along the open or channeling directions of the surface lattice, corresponding to the $\phi = \pm 30°$ azimuths. These are directions along which an ejecting atom is guided outwards rather than being blocked by neighboring atoms, as would occur along close-packed azimuths. At low KE, the azimuthal ejection distribution exhibits threefold symmetry (i.e., the intensities along $\pm 30°$ are inequivalent), whereas at high KE it exhibits approximately sixfold symmetry (i.e., the intensities along $\pm 30°$ are almost equal). Evidently, ejection mechanisms giving rise to high KE atoms involve only the first layer, leading to sixfold symmetry. By contrast, ejection mechanisms giving rise to low KE atoms involve collisions with more than just the first layer, leading to threefold symmetry. By comparing the EARN data from clean Rh{111} to the calculated distributions and to the known surface structure, the role of this structure in dictating ejection distributions is thus clarified.

The EARN data from oxygen-covered Rh{111} exhibit distinct differences when compared to those obtained from clean Rh{111}. First, the intensity of Rh atom ejection is reduced by the presence of the oxygen overlayer, especially in the off-normal direction. Second, ejection along the $\phi = -30°$ azimuth is reduced more than ejection along the $\phi = +30°$ azimuth. Third, the polar angle at which off-normal ejection maximizes is 2°–10° closer to the surface normal compared to the EARN data from clean Rh{111}. Using the idea that surface channeling and blocking of ejecting atoms is responsible for determining ejection distributions, the changes that occur upon oxygen adsorption can be interpreted in terms of blocking of escaping Rh atoms by oxygen adatoms bound in particular surface sites.[5–7] A simple analysis would be that if oxygen atoms bind in the C sites, they

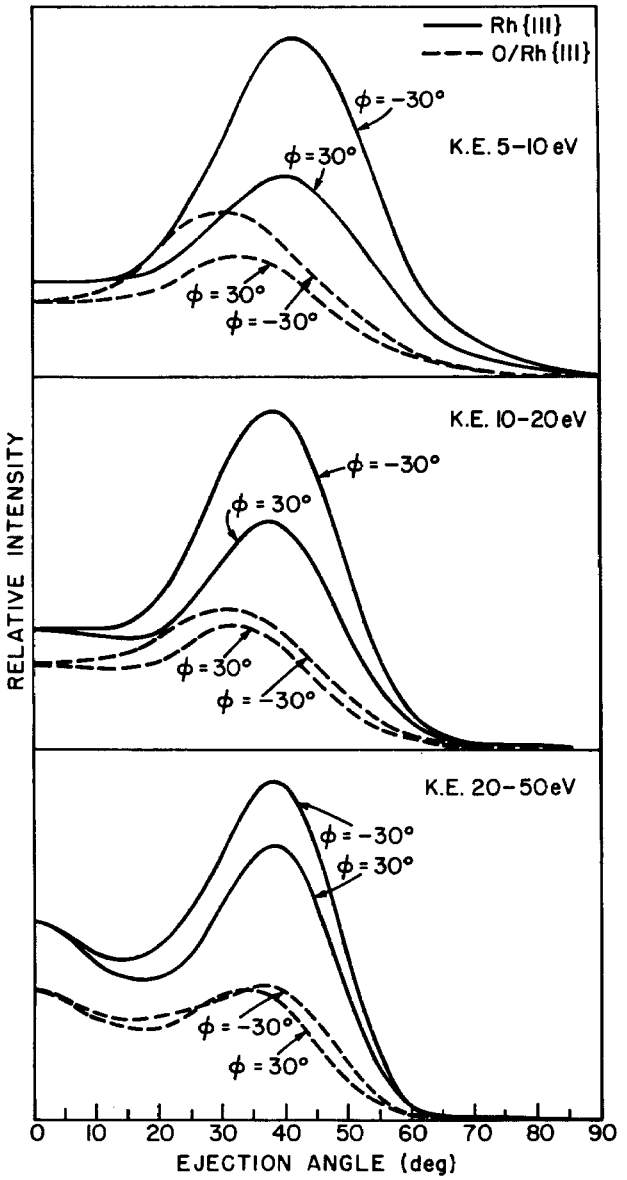

FIG. 2. Experimental polar angular distributions of Rh atoms ejected from clean and oxygen-covered Rh{111}. A polar angle of $\theta = 0°$ corresponds to normal ejection from the sample surface. The oxygen coverage displays a $p(2\times2)$ LEED pattern.

would preferentially block Rh atoms escaping along the $\phi = -30°$ azimuthal direction. A dynamical LEED study indicates that oxygen binds 1.23 Å above threefold hollows.[21] If this adatom geometry is correct, blocking by oxygen atoms would have a maximum effect at a Rh ejection angle of $\theta \sim 40°$. The shift in peak polar angle of ejection upon oxygen adsorption would be explained by the tendency of oxygen atoms to deflect escaping Rh atoms closer to the normal direction.[7]

The KE spectra of Rh atoms ejected from both clean and oxygen-covered Rh{111} are shown in Fig. 3. KE spectra were measured along three different ejection directions: the normal direction, $\theta = 0°$, and two off-normal directions, $\theta = 45°$, characterized by the azimuths $\phi = -30°$ and $\phi = 30°$, respectively. The polar angle of 45° was chosen as a compromise among the peak positions for the various

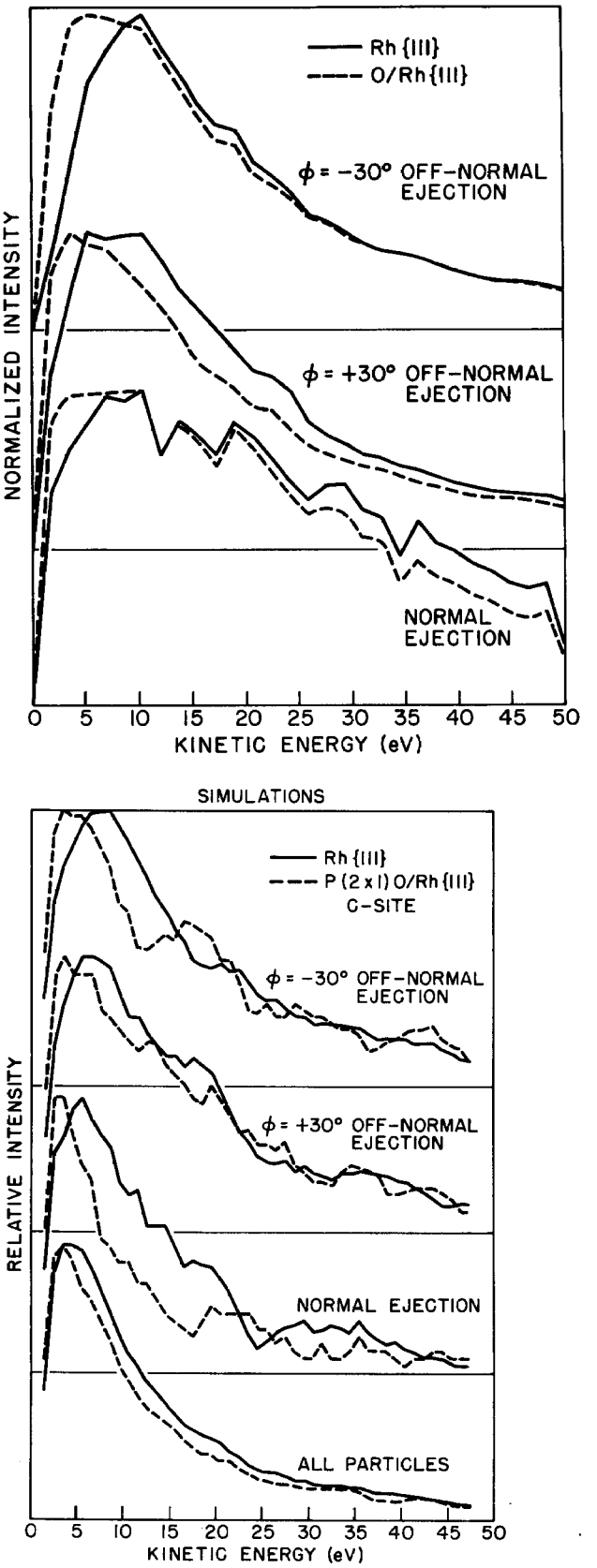

FIG. 3. (a) Experimental kinetic energy distributions of Rh atoms ejected from clean and oxygen-covered Rh{111}, taken at ejection angle $\theta = 45°$. $p(2\times2)$ LEED pattern was observed for the oxygen overlayer. The data are normalized to the same peak signal intensity. The polar angle resolution is $\pm 3°$. (b) Simulated kinetic energy distributions of Rh atoms ejected from clean Rh{111} and $p(2\times1)$O/Rh{111}, taken at ejection angle $\theta = 40°$. The polar angle resolution is $\pm 10°$.

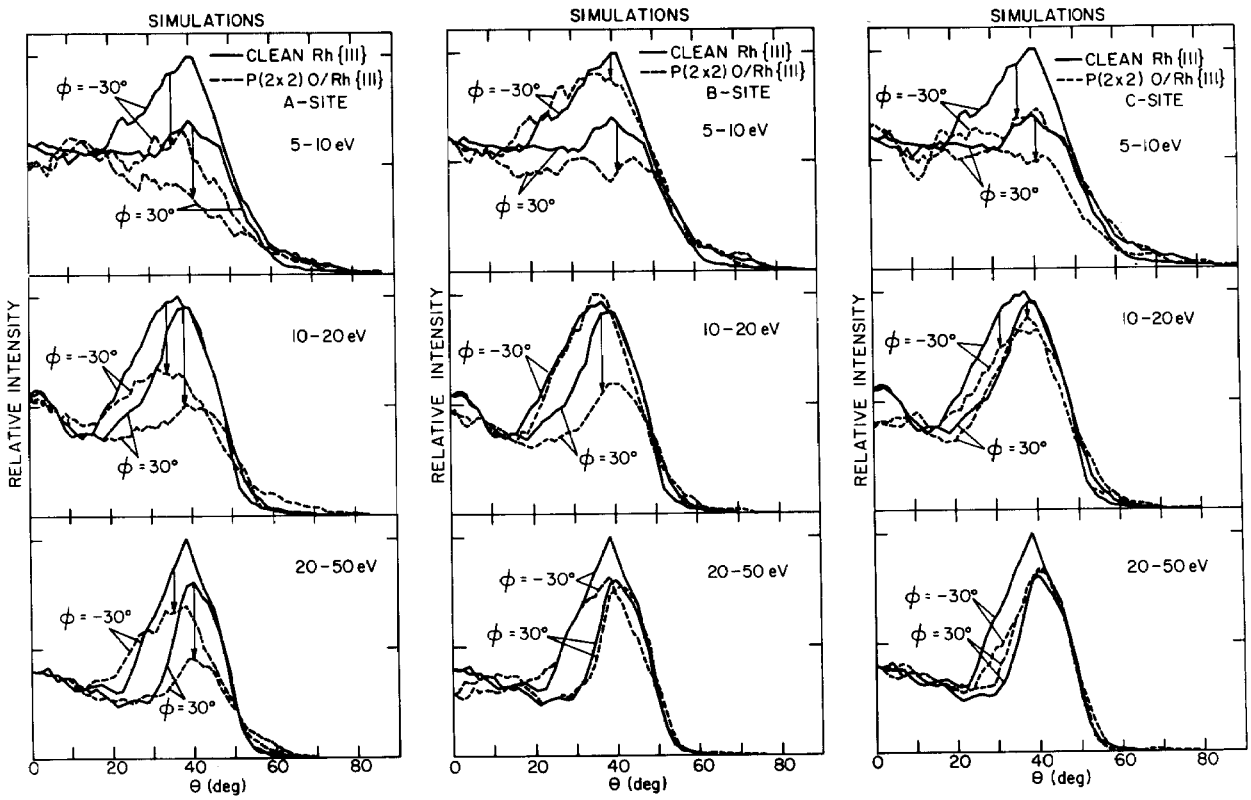

FIG. 4. Simulated polar angular distributions of Rh atoms ejected from clean Rh{111} and $p(2\times2)$O/Rh{111} as a function of the energy of the ejected Rh atoms.

oxygen coverages and Rh atom KE ranges. Adsorption of oxygen corresponding to a LEED (2×2) pattern causes the peaks of the KE spectra to be shifted by about 2–5 eV to lower KE. Analytical models of collison cascade desorption predict that the KE corresponding to the peak in the KE spectrum is proportional to the surface binding energy.[32–34] Using this interpretation the data presented here suggest that oxygen may reduce the binding energy of Rh atoms to the oxygen covered Rh surface from the clean surface value. Alternately the collisional blocking by the oxygen overlayer may cause the peak to shift downward. As we shall see from the comparison to calculations, it is this latter explanation which we believe to be valid. This downward shift in the peaks of the KE spectra contrasts with results obtained by less sensitive techniques such as Doppler shift laser fluorescence spectroscopy (DSLFS), in which samples must be significantly eroded by incident ions in order to obtain good signal to noise ratios. In such experiments, oxygen overlayers must be maintained by exposing the surface to oxygen as it is eroded. The peaks in the KE distributions shift upwards in energy by a factor of 1.5–2.0 under these dynamic desorption conditions.[34]

The results from the classical dynamics calculations of desorption from both clean Rh{111} and from the $p(2\times2)$ O/Rh{111} system for the three adsorption sites characterized by a coverage of 0.25 ML are shown in Fig. 4. On the clean surface, the dominance of ejection along the $\phi = -30°$ azimuth allows us to identify that azimuth on the crystal sample. For each of the three assumed binding sites, the calculated Rh atom ejection yield is reduced least in the high KE range, as expected since the interaction cross section between Rh and O decreases for higher relative KE. If the oxygen atoms are assumed to bind in the *A* site, then the signal along the $\phi = 30°$ azimuth is reduced relatively more than the signal along the $\phi = -30°$ azimuth, in contradiction to the data. If the oxygen atom binds in the *B* site, then the same relative effect is seen in the 5–20 eV KE range, again in contradiction to the data. However, if oxygen binds in the *C* site, the signal along the $\phi = 30°$ azimuth is reduced relatively more than the signal along the $\phi = 30°$ azimuth, for all KE ranges shown. The assumption of the *C* site results in calculated ejection distributions which are in qualitative agreement with the data shown in Fig. 2. On the other hand, the calculated change in ejection yield with oxygen coverage in any site is very small. In the experiment the difference in yield is about a factor of 2 between the clean and oxygen covered surface.

The results from the classical dynamics calculation of desorption from the $p(2\times1)$ O/Rh{111} system characterized by a coverage of 0.50 ML are shown in Fig. 5. If oxygen atoms are assumed to bind in the *A* sites, the ejection signals along the $\phi = \pm 30°$ azimuths are reduced to about the same size. If oxygen atoms are assumed to bind in the *B* sites, then the signal is clearly more reduced along the $\phi = 30°$ azimuth than along the $\phi = -30°$ azimuth, especially for KE greater than 10 eV. This trend is opposite to what is observed in the data, which show preferential reduction of signal measured along the $\phi = -30°$ azimuthal direction upon oxygen ad-

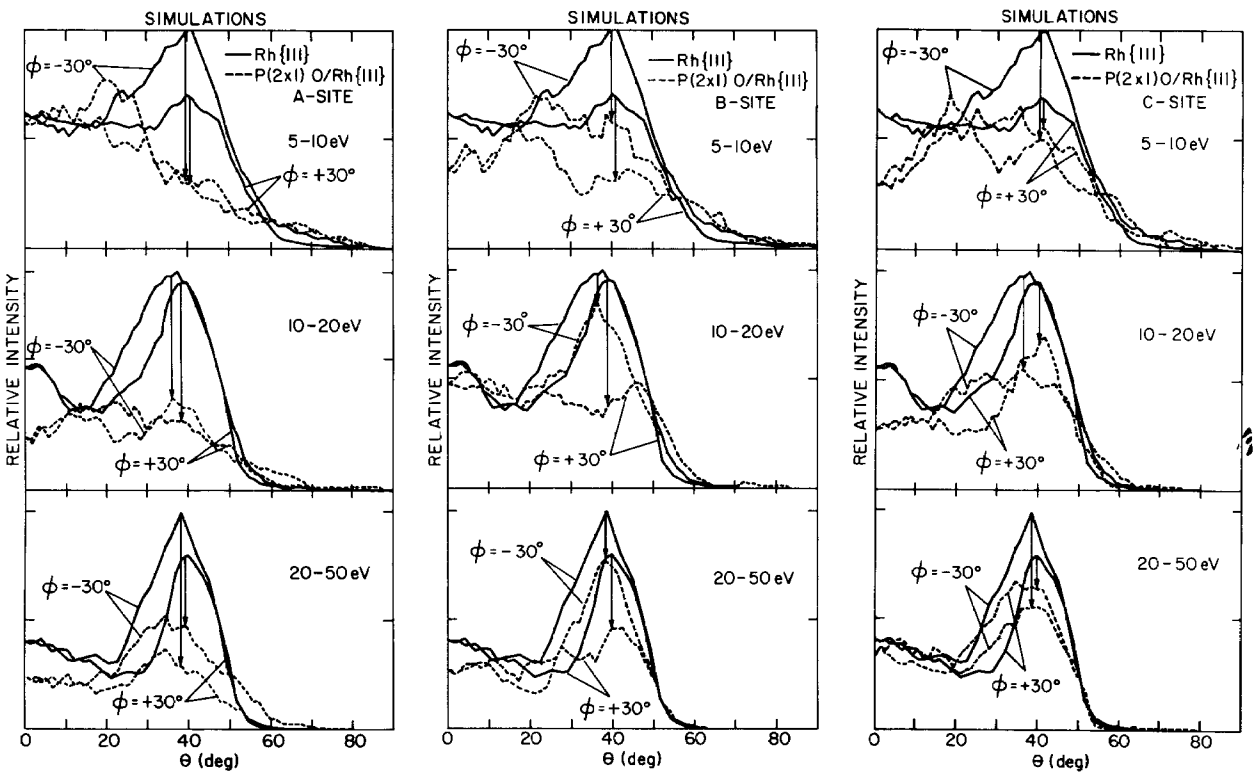

FIG. 5. Simulated polar angular distributions of Rh atoms ejected from clean Rh{111} and $p(2\times1)$O/Rh{111}.

sorption. Finally, if the oxygen atoms are assumed to bind in the *C* sites, then for all KE ranges there is a greater reduction in the signal along the $\phi = -30°$ azimuth than along the $\phi = +30°$ azimuth. Thus, the assumption of the *C* site and a 0.5 ML coverage leads to good agreement between calculated ejection distributions and data in the KE range above 10 eV. It is seen that detailed classical dynamics calculations confirm the tentative conclusion that oxygen atoms bind in the *C* site,[5–7,21] and affect the Rh atom ejection distributions through directionally preferential blocking. There even appears to be a slight shift in the peak position towards the surface normal. It should be noted that in the studies of the polar distributions of clean Rh{111} deficiencies in the EAM potential were observed when describing the ejection of the low ($\leqslant$10 eV) energy particles.[8] Similar difficulties exist for the oxygen overlayer configuration. We place most confidence then, on the results obtained at $\geqslant$10 eV.

The calculated energy distributions at specific polar angles are shown in Fig. 3(b) for comparison with the experimental curves. The downward shift in peak position observed in the experimental curves is reproduced in the calculated curves. Analytic models of sputtering state that the peak in the energy distribution should be proportional to the binding energy of the atom to the substrate.[32,33,35,36] In the calculations the Rh surface atoms are bound by $\sim$5.1 eV in clean Rh{111} and $\sim$5.9 eV if oxygen is present. The attraction of a surface metal atom to the other metal atoms via the EAM potential is independent of the presence of the oxygen atoms. Since the pair interaction with the oxygen atoms increases the binding energy and if the concepts from the analytic model were correct, the peak in the energy distribution should shift to a higher value upon oxygen adsorption. This is contrary to what is observed. Our results suggest, then, that the Rh atoms lose kinetic energy as they eject due to collisions with overlayer atoms, causing the peak position to be reduced from that of the clean surface. For systems involving overlayers, then, the peak position in the energy distribution is related not only to the binding energy of the atom to the surface, but also to the magnitude of collisional energy losses. These shifts in peak position are not found to be significantly related to the binding site of the overlayer atom.

The downward trend we observe in our KE ejection distributions upon oxygen adsorption is opposite to what is observed in experiments in which surfaces are simultaneously exposed to oxygen and to a high flux of eroding incident ions. In these experiments, KE spectra of ground state metal atoms are shifted by 5–10 eV to higher KE.[37] This outward energy shift points to a difference in the chemistry of bonding between a chemisorbed $p(2\times1)$ oxygen overlayer and an oxide, the latter additionally being heavily influenced by ion-beam-induced mixing and surface roughness. One mechanism that has been proposed to account for the broadening of the KE distributions is creation of metal–oxide quasimolecules, collisional excitation of these molecules, and subsequent branching to excited, repulsive electronic states which give rise to a variety of ejected excited and ground state metal and oxygen atoms.[37,38] However, the surface binding energy of ionic oxides has been shown to be quite large when vacancy and electronic defect formation energies are properly taken into account,[39] leading to an alternate explanation of these broadened KE distributions. The exper-

iment discussed in the present paper seems to be the only existing study in which KE distributions are measured on oxygen-exposed surfaces under low ion beam fluence conditions characterized by negligible ion-beam-induced damage or mixing of surface constituents. It would be extremely interesting to generate a Rh–oxide film in a high pressure cell, and then subject the resulting film to our "static" EARN measurement in order to see if the outward shift in the KE distributions persists under well-defined conditions. A comparison of KE spectra taken under conditions of low ion damage and for a wide range of oxygen coverage and chemical binding situations would provide useful information on this interesting aspect of oxidation of metals. The EARN technique may also be employed to selectively detect excited atoms, making possible a detailed study of how oxygen layers influence excited state atom ejection yields and distributions.

V. CONCLUSION

Angular distributions of keV ion desorbed atoms from single crystal surfaces reflect the structure of the surface through channeling and blocking phenomena. This structural sensitivity has been demonstrated convincingly by energy- and angle-resolved measurements of desorbed neutral atoms and by classical dynamics calculations of the desorption event, which enhance our ability to interpret ejection data. Channeling and blocking of desorbed atoms provide a uniquely simple yet powerful means for determining the location of adatoms based on their effects on the desorption patterns of the underlying substrate atoms. We have studied the (2×2)–O/Rh{111} system extensively, and we have determined that oxygen atoms bind in the C sites, which are threefold hollows above third layer Rh atoms. We have also noted that the calculations best match the data when an oxygen coverage of 0.5 ML is assumed, confirming independent results suggesting that the oxygen coverage on the (2×2)–O/Rh{111} system is higher[15–17] than is commonly assumed.[5–7,21] Independent experiments are underway in our group to calibrate the oxygen coverage of the chemisorbed O–Rh{111} system. The peak in energy distribution of ejected Rh atoms from the oxygen covered surface is at a lower energy value than that of the clean metal. This indicates that collisional energy loss processes contribute to determining the peak position as well as the well known binding energy effect.

ACKNOWLEDGMENTS

The financial support of the Office of Naval Research, the National Science Foundation, the Shell Development Company, and the IBM Program for the Support of the Materials and Processing Sciences is gratefully acknowledged. One of us (B.J.G.) thanks the Camille and Henry Dreyfus Foundation for additional support. The Pennsylvania State University supplied a generous grant of computer time for these studies.

[1]N. Winograd, Prog. Solid State Chem. **13**, 285 (1982).
[2]C.-C. Chang, G. P. Malafsky, and N. Winograd, J. Vac. Sci. Technol. A **5**, 981 (1987).
[3]R. Blumenthal, S. K. Donner, J. L. Herman, R. Trehan, K. P. Caffey, E. Furman, N. Winograd, and B. D. Weaver, J. Vac. Sci. Technol. B **6**, 1444 (1988).
[4]C.-C. Chang and N. Winograd, Phys. Rev. B (in press).
[5]N. Winograd, P. H. Kobrin, G. A. Schick, J. Singh, J. P. Baxter, and B. J. Garrison, Surf. Sci. **176**, L817 (1986).
[6]B. J. Garrison, C. T. Reimann, N. Winograd, and D. E. Harrison, Jr., Phys. Rev. B **36**, 3516 (1987).
[7]J. Singh, C. T. Reimann, J. P. Baxter, G. A. Schick, P. H. Kobrin, B. J. Garrison, and N. Winograd, J. Vac. Sci. Technol. A **5**, 1191 (1987).
[8]B. J. Garrison, N. Winograd, D. M. Deaven, C. T. Reimann, D. Y. Lo, T. A. Tombrello, D. E. Harrison, Jr., and M. H. Shapiro, Phys. Rev. B **37**, 7197 (1988).
[9]S. P. Holland, B. J. Garrison, and N. Winograd, Phys. Rev. Lett. **43**, 220 (1979).
[10]D. W. Moon, N. Winograd, and B. J. Garrison, Chem. Phys. Lett. **114**, 237 (1985).
[11]F. M. Kimock, J. P. Baxter, and N. Winograd, Surf. Sci. **124**, L41 (1983).
[12]B. J. Garrison and N. Winograd, Science **216**, 805 (1982).
[13]P. H. Kobrin, G. A. Schick, J. P. Baxter, and N. Winograd, Rev. Sci. Instrum. **57**, 1354 (1986).
[14]D. G. Castner, B. A. Sexton, and G. A. Somorjai, Surf. Sci. **71**, 519 (1978).
[15]T. Matsushima, Surf. Sci. **157**, 297 (1985).
[16]D. G. Castner and G. A. Somorjai, Appl. Surf. Sci. **6**, 29 (1980).
[17]T. W. Root, L. D. Schmidt, and G. B. Fisher, Surf. Sci. **134**, 30 (1983).
[18]J. L. Gland, Surf. Sci. **93**, 487 (1980).
[19]T. Narusawa, W. M. Gibson, and E. Törnqvist, Phys. Rev. Lett. **47**, 417 (1981).
[20]C.-M. Chan and W. H. Weinberg, J. Chem. Phys. **71**, 2788 (1979).
[21]P. C. Wong, K. C. Hui, M. Y. Zhou, and K. A. R. Mitchell, Surf. Sci. **165**, L21 (1986).
[22]L. A. DeLouise and N. Winograd, Surf. Sci. **138**, 417 (1984).
[23]C. M. Mate and G. A. Somorjai, Surf. Sci. **160**, 542 (1985).
[24]H. H. Andersen and H. L. Bay, in *Sputtering by Particle Bombardment I*, edited by R. Berisch (Springer, Berlin, 1981), p. 145.
[25]M. S. Daw and M. I. Baskes, Phys. Rev. Lett. **50**, 1285 (1983).
[26]M. S. Daw and M. I. Baskes, Phys. Rev. B **29**, 6443 (1984).
[27]M. Manninen, Phys. Rev. B **34**, 8486 (1986).
[28]M. W. Finnis and J. E. Sinclair, Philos. Mag. A **50**, 45 (1984).
[29]I. M. Torrens, *Interatomic Potentials* (Academic, New York, 1972).
[30]P. A. Thiel, J. T. Yates, Jr., and W. H. Weinberg, Surf. Sci. **82**, 22 (1979).
[31]K. A. R. Mitchell, Surf. Sci. **149**, 93 (1985).
[32]M. W. Thompson, Philos. Mag. **18**, 377 (1968).
[33]B. J. Garrison, N. Winograd, D. Lo, T. A. Tombrello, M. H. Shapiro, and D. E. Harrison, Jr., Surf. Sci. **180**, L129 (1987).
[34]W. Husinsky, P. Wurz, B. Strehl, and G. Betz, Nucl. Instrum. Methods Phys. Res. B **18**, 452 (1987).
[35]J. P. Baxter, J. Singh, G. A. Schick, P. H. Kobrin, and N. Winograd, Nucl. Instrum. Methods B **17**, 300 (1986).
[36]B. J. Garrison, Nucl. Instrum. Methods B **17**, 305 (1986).
[37]W. Husinsky, J. Vac. Sci. Technol. B **3**, 1546 (1985).
[38]G. Blaise, Surf. Sci. **60**, 65 (1976).
[39]R. Kelly, Nucl. Instrum. Methods B **18**, 388 (1987).